Measured Stark widths of several spectral lines of Pb III

A. Alonso-Medina

Departamento de Física Aplicada, EUIT Industrial, Universidad Politécnica de Madrid, Spain
Ronda de Valencia 3, 28012 Madrid, Spain

A B S T R A C T

The Stark full widths at half of the maximal line intensity (FWHM, ω) have been measured for 25 spectral lines of Pb III (15 measured for the first time) arising from the $5d^{10}6s8s$, $5d^{10}6s7p$, $5d^{10}6s5f$ and $5d^{10}6s5g$ electronic configurations, in a lead plasma produced by ablation with a Nd:YAG laser. The optical emission spectroscopy from a laser-induced plasma generated by a 10 640 Å radiation, with an irradiance of 2×10^{10}W cm^{-2} on a lead target (99.99% purity) in an atmosphere of argon was analysed in the wavelength interval between 2000 and 7000 Å. The broadening parameters were obtained with the target placed in argon atmosphere at 6 Torr and 400 ns after each laser light pulse, which provides appropriate measurement conditions. A Boltzmann plot was used to obtain the plasma temperature (21,400 K) and published values of the Stark widths in Pb I, Pb II and Pb III to obtain the electron number density (7×10^{16}cm^{-3}); with these values, the plasma composition was determined by means of the Saha equation. Local Thermodynamic Equilibrium (LTE) conditions and plasma homogeneity has been checked. Special attention was dedicated to the possible self-absorption of the different transitions. Comparison of the new results with recent available data is also presented.

Keywords:
Laser-produced plasma
Line profile
Stark width
Atomic data
Lead

1. Introduction

Stark broadening of ion and atom spectral lines is relevant not only for atomic structure research, but also for applications to astrophysics and analytical techniques for plasma diagnosis. An interest in the determination of radiative constants of doubly ionized lead has been produced, this is so not only because the analysis of astrophysical data, but also because accurate values of these parameters are of interest for atomic structure studies. Recently, interest in Pb III has increased because of its spectral lines identified in the spectrum of the chemically peculiar B-type star χ Lupy [1,2] and of hot subdwarf B (sdB) stars [3] with the Goddard High Resolution Spectrograph on the Hubble Space Telescope.

The previous works, published in literature, about the Stark widths of Pb III are scarce. In 2007 in work [4], has been measured in a laser-induced plasma (LIP) (at an temperature of 25,200 K and an electron number density of 10^{17} cm^{-3}), and a lead target in an argon atmosphere at 12 Torr, Stark widths of 10 spectral lines that belong to 6s7s–6s7p, 6s6d–6s7p and $6p^2$–6s7p transition of Pb III. Semi-classical approximate values of the Stark parameters for 122 spectral lines of Pb III arising from $5d^{10}$ 6sns (n = 6,7), $5d^{10}$ 6snp (n = 6–8) and $5d^{10}$ 6snd (n = 6,7) configuration have been calculated using a set of wave function obtained from Hartree–Fork relativistic calculations [5]. In a recent work [6] we have calculated values of the Stark broadening parameters for 30 spectral lines of Pb III arising from $5d^{10}$ 6snp (n = 6–8), $5d^{10}$ 6s5f and $5d^{10}$ 6sng (n = 5,6) configurations using a semi-classical approach and the introduction of the terms that allow us to take into account the Core Polarization (CP) effects, where Stark widths are presented as functions of temperature and for an electron density of 10^{23} m^{-3}.

In the present work, Stark widths in Pb III, have been obtained experimentally using laser-induced breakdown spectroscopy (LIBS). The source of free lead atoms and ions in different stages of ionization is a laser-produced plasma, and the aim of this work is to provide some new experimental values of several Stark widths of Pb III, comparison with the theoretical results in the recent work [6] and verify the experimental values obtained in Ref. [4]. In this paper, a plasma generated by focusing a laser beam on a sample of lead in an argon atmosphere at 6 Torr and 400 ns after each laser light pulse, which provides appropriate measurement conditions, has been used in order to provide Stark widths (FWHM) of 25 Pb III spectral lines corresponding to the $5d^{10}$ 6s8s, $5d^{10}$ 6s7p, $5d^{10}$ 6s5f and $5d^{10}$ 6s5g configurations (15 measured for the first time), between 2000 and 7000 Å, have been measured by determining the line profiles and the emission line intensity. Special attention was paid to the possible self-absorption of the different transition. The possible contribution from other broadening mechanisms (see, such as natural broadening, resonance broadening, van der Waals broadening and Doppler broadening) was also taken into account.

A study has been made of the temperature (21,400 K), the electron number density (7×10^{16}cm^{-3}) and the plasma homogeneity. The state of local thermodynamic equilibrium (LTE) has been also discussed, since as is well known, the classical approach in the study of laser-produced plasma is based on the assumption of LTE [7].

2. Experimental details

The experimental system it has already been described in previous papers [4,8–11], a more detailed description is presented in [10,11]; nevertheless, we shall explain it here briefly.

Briefly, the system consists of a Q-switched Nd:YAG laser that generates 290 mJ pulses of 7 ns of duration at a frequency of 20 Hz and a wavelength of 1064 ns and 1 m Czerny–Turner spectrometer, range 1900 to 7000 Å, with a 2400 grooves/mm holographic grating and a 50 μm external slit, equipped with a gated optical multichannel analyser (OMA III EG&G, formed by 1024 silicon photodiodes), which allowed the detection of each spectrum and its digital recording for later numerical analysis. The linear dispersion of spectrometer to small scattering angles, is 4.17 Å/mm. This linear dispersion means a dispersion of 0.1 Å/channel, taking into account the size of 25 μm of each of the 1024 photodiodes of OMA. The spectral band detected by the photodiode array is about 100 Å. However the actual values depend on the wavelength, i.e. the scattering angle. In our case we have dispersions of 0.1043 Å/channel for 1900 Å to 0.0584 Å/channel for 7000 Å.

The computer has a card used for communications, through which the communication is made with the central unit OMA. From this computer has been programmed the whole process of acquisition of data from the OMA and has been received the spectrum, after the end throughout the measurement process. It has a time resolution, with a minimum duration of the time window of 100–200 ns, and the spectral band detected by the device is about 100 Å. The resolution of the spectroscopic system was 0.36 Å in first order.

A chamber was used to generate the plasma on a gas atmosphere. A previous vacuum of 10^{-5} Torr was attained inside the chamber by means of a turbomolecular pump, and it was filled with argon and maintained at a constant pressure throughout the measurements, using a small continuous flow of gas to maintain the purity of the atmosphere. The temperature, electron number density and time evolution of laser-produced plasma can be controlled. Samples were located inside the chamber, on top of a device capable of moving it horizontally with respect to the laser beam, focused in such a way that the plasma was formed in each measurement on the smooth surface of the target and not on the crater formed during the previous measurement, this could influence the intensity of the spectral lines and could lead to the destruction of the sample. Following several tests, the broadening parameters were obtained with the target placed in argon atmosphere at 6 Torr, which provides appropriate measurement conditions.

The laser light was focused at right angle onto the sample with a 12 cm focal length lens. The laser irradiance on the blank was 2×10^{10} W cm^{-2}. The spot size, measured at the target surface, was a circle of diameter 0.5 mm. It features a quartz window that lets through light that is sent to the spectrometer entrance slit, located 8 cm from the plasma.

The temporal history of the plasma is obtained by recording the emission features at predetermined delays and at a fixed gate width. The measurements were repeated at several delay times (150 to 900 ns) and at a fixed gate time of 100 ns. The measurements consist in the accumulation of 20 laser pulses at a delay time and were obtained, after ablative cleaning the target with 2 laser pulses in order to remove impurities. To obtain the best signal to noise ratio, the measurements of spectral lines of Pb III were made with a delay of 400 ns, and the recording interval was 100 ns. Fig. 1 presents three sections of spectra, in the range of 3630 to 3700 Å, and time resolved emission spectra at six delays: 300, 400, 600 and 900 ns from laser-produced plasma: a) in vacuum, b) in a 6 Torr argon atmosphere and c) in a 12 Torr argon atmosphere. In vacuum some of the spectral lines of Pb I can be observed and in an argon atmosphere besides the spectral lines of Pb I, some Pb III lines can be observed. It is considered that, a 6 Torr argon atmosphere and a delay of 400 ns, are appropriate measurement conditions of spectral lines of Pb III.

Relative spectral response calibration of the experimental system (spectrometer plus OMA) was made using a calibrated deuterium lamp (for the 1900–4000 Å) range and calibrated tungsten lamp (for the 3500–7000 Å range). The final calibration test was the result of the overlapping joint regions of these two lamps, and employing a least-square fitting process. The system efficiency was measured five times, and the error was estimated to be around 5%.

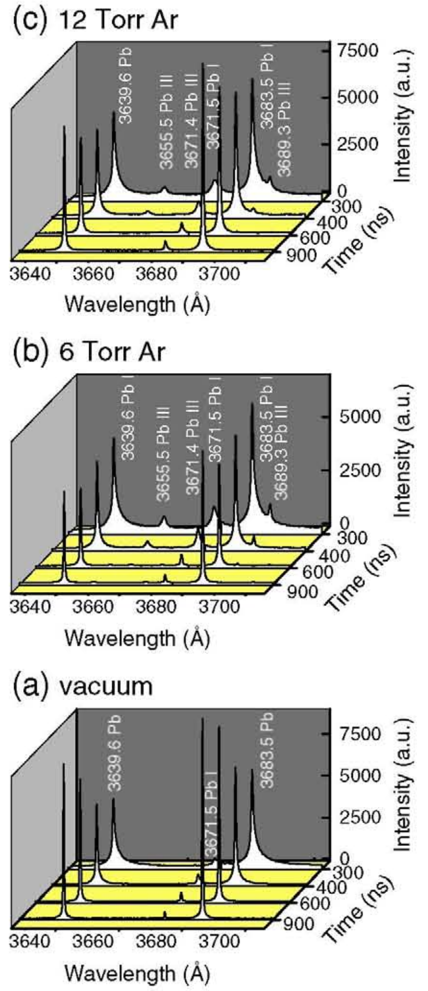

Fig. 1. (a), (b) and (c). Emission spectral lines, in range 3630–3700 Å, obtained for lead ablation at four delays: 300, 400, 600 and 900 ns. (a) in vacuum, (b) in a 6 Torr argon atmosphere, (c) in a 12 Torr argon atmosphere.

The same experimental system was used to study the homogeneity of the plasma, but in order to have spatial resolution, the light was focused by means of a lens on a 1 mm light guide being able to select the point of the plasma from which the light emission was observed. The lens and optical fiber connector have been mounted on a telescopic spring that allows one to vary their relative distance to coincide with the focus distance of the image of the plasma, keeping the plasma-lens-optical fiber aligned. The support wass mounted on an optical bench, allowing movement horizontally and vertically in a controlled manner, thereby varying the area of plasma whose image is detected in the optical fiber, see schematic in Fig. 1 of Ref. [9]. The measurement were taken by scanning the plasma emission in two perpendicular directions; through the axis of the plasma with a distance from the blank in the 0.25–2.75 mm range to study the evolution of the plasma in space, and parallel to the surface of the target with a radial distance in the range of 0–1.12 mm, to determine where the different lead atomic species are located in the plasma and to determine the real values of the parameters of the plasma (intensities, widths of spectral lines, temperature and electron number density) [9,12].

The spectra were stored in a computer for further analysis and treated by software which is able to separate two close overlapping lines and to determine their relative intensities, with uncertainties$\leq$3%. The analysis of the spectral lines was made by fitting the observed line shapes to numerically generated Voigt profiles and, with them, make the deconvolution to obtain the Lorentzian and Gaussian profiles, Lorentzian profile from Stark broadening, with Gaussian profile from Doppler broadening and instrumental broadening. The instrumental profile needed for the numerical analysis of each spectrum was determined from the observation of several narrow spectral lines emitted by hollow-cathode lamp. This profile has been a Voigt profile FWHM = 0.24 Å , Gaussian FWHM = 0.17 Å and Lorentzian FWHM = 0.11 Å for a wavelength of 3000 Å, and the estimated error of this measurement was about 3%.

The absorption effects were calculated taking into account the temperature and electron density of the plasma. An estimation of the absorption coefficient of all the lines studied will be shown in a later discussion, in order to verify that self-absorption was negligible. In this paper, self-absorption effects turned out to be lower than 1% for most intense lines. Thus, the plasma can be considered optically thin.

3. Line width measurement

As is well known, the shape and width of the spectral lines emitted by plasma are governed by collisional processes perturbing the emitting atoms and ions.

When lines widths (FWHM, ω) are concerned, the problem is complicated, as it is necessary then to separate different effects that influence the experimental profile. In this work we have undertaken a study of the contributions of different broadening mechanisms. To deduce the line FWHM (ω) we fitted each of the recorded lines by a Voigt profile, which has been corrected for instrumental (spectrometer + OMA, ω_i) broadening. The Voigt type due to the convolution of the Lorentzian Stark (ω_S) and Gaussian (ω_g), profiles caused by Doppler effects. For the electron number density and temperature in our experiment, the Lorentzian fraction was significant.

The Lorentzian part, ω_l, of the line profile is: the natural width (ω_N), the resonance broadening (ω_R), the van der Waals (ω_V) and the Stark broadening (ω_S).

$$\omega_l = \omega_N + \omega_R + \omega_V + \omega_S \tag{1}$$

Nevertheless, the orders of magnitudes given for the studied lines, show that the lorentzian part, ω_l, of the line profile is dominated by the Stark effect.

The natural width arises because even an unperturbed level has a finite lifetime due to spontaneous emission. [13–15]. For the studied Pb III lines ω_N is of the order of 10^{-6} Å and is negligible in comparison with the widths measured experimentally for plasma-induced laser.

Resonance broadening (ω_R) results from the collision with energy exchange between two identical particles, but in different levels, if one of the levels connected by the transition is the ground state, ω_R (FWHM) can be estimated by the formula [13,16–18]:

$$\omega_R \cong 0.368 \times 10^{-7} \left(\frac{g_1}{g_R}\right)^{\frac{1}{2}} f_R \ \frac{N}{c} \ \lambda^2 \lambda_R \ [nm] \tag{2}$$

where λ is the wavelength of the observed radiation and λ_R is the resonance wavelengths, f_R is the absorption oscillator strength of the upper level of resonance transition, g_1 and g_R are the statistic weights of the ground state and the upper resonance level, respectively, c the speed of light and N is the number density of ground state particles which are the same species as the emitter. For the Pb III lines is of the order of 10^{-5} Å at a density of 7×10^{16} cm^{-3}. Here we assumed largest N possible, i.e. presence of doubly charged Pb ions only.

The van der Waals broadening results from the dipole interaction of an excited atom with the induce dipole of a neutral ground-state atom of density Ne. Using Griem's estimate [13,14] even in this case, it is usually negligible (of the order of 10^{-6} Å).

For a Doppler broadened spectral line the intensity distribution is gaussian whose, ω_D, is given by a simple equation based on the Maxwellian distribution [12,14]:

$$\omega_D = \lambda_0 \sqrt{\frac{8kT \ ln2}{Mc^2}} \tag{3}$$

where λ_0 (m) is the wavelength at the centre of the absorption line, k(J/K) the Boltzmann constant, T(K) the absolute temperature, M(kg) the atomic mass and c(m/s) the speed of light. An example, at a temperature of 21,400 K, the Doppler width is estimated to be 3×10^{-4} Å for the transition at 3655.5 Å of Pb III. In the present work, compared with the total line widths, Doppler effects can be ignored.

As mentioned above, the instrumental broadening (ω_i) was determined previously from the analysis of narrow spectral lines from hollow-cathode lamps, resulting to be a Voigt profile.

To fit the emission line profiles in the analysis and obtain the FWHM, we used a software tool that is able to numerically generate Voigt profiles by an analytical the experimental profiles. The tool allows the user to modify, among others, some line parameters such as the width (in channels) before and after subtracting the contribution of the instrumental profile, and the Gaussian and Lorentzian components. It also provides the ability to subtract background noise linearly. The Stark broadening has been directly obtained as the Lorentzian part of the Voigt function.

The fitting of the observed profiles provides the broadening of the spectral lines, as well as the total intensity very accurately. Any line, that has been measured in this work, was isolated enough to consider that the fitting procedure of the wings was correct. For the plasma diagnostics, the area under each line profile from the aforementioned fitting represents the relative intensity.

4. Results and discussion

4.1. Determination of plasma temperature and electron number density

The plasma temperature was measured by means of a using the Boltzmann plot method for determining the excitation temperature, and Saha's equation was used for determining the ionization temperature. It is well known that LTE plasmas are characterized by single temperature [13–15,19], recently Cristoforetti et al [20] conducted a detailed study.

The excitation temperature has been determined by means of a Boltzmann plot using seven Pb III lines (at wavelengths, 4798.6, 4761.1, 3854.1, 3728.7, 3689.3, 3530.2 and 3137.8 Å NIST [21]) obtaining 21,400 ± 700 K for ΔE = 1.367 eV. All the data exhibited a linear fit with a correlation coefficient better than 0.998. This value has been obtained from the relative intensities required for applying this method, obtained using laser-produced plasma in this work, and the transition probabilities are taken from reference [10]. The energies of the different levels are those of Moore [22]. The relative uncertainty were estimated from the standard deviation of the slopes obtained in the least squares fittings; the uncertainties that are taken into account are: (a) the line profile fitting procedure (~1%), (b) the relative line intensity determination (~2%) and (c) the transition probabilities (9.7–10.9%, depending on each line) [10], see Table 1.

The ionization temperature was calculated using the relative line intensity ratio method (in the electron density 7×10^{16} cm^{-3}), [12–14], using Pb II (3718.3 Å) and Pb III (3854.1 Å) spectral lines; the necessary atomic data are taken from Ref. [10,23,24]. The value obtained is 21,200 K with an estimated error of ~10%. The reason for selecting these lines is that the self-absorption does not appear.

These values, the excitation temperature and the ionization temperature, are totally compatible and are close to 21,400 K, justifying the existence of LTE.

Stark broadened spectral line widths depend on the electron density. The FWHM of Stark broadening profile is related with the electron number density through the following expression [13,19,25]:

$$\omega = 2\omega_p\left(\frac{N_e}{10^{16}}\right)\left[1 + 1.75A\left(\frac{N_e}{10^{16}}\right)^{1/4}\left(1-1.2N_D^{-1/3}\right)\right] \quad (4)$$

where ω (in Å) is the FWHM of the transition considered and obtained at the density N_e expressed in cm^{-3}. The coefficients ω_p and A, both independent of density and weak functions of temperature, are the electron impact-width parameter and the ion-broadening parameter, respectively. The parameter N_D is the number of particles in the Debye sphere, which must be in excess of the lower limit $N_D = 2$ of the Debye approximation for correlation effects, see Wolf [26]. For the electron densities present in this study, the quasi-static ion broadening, taken into account in the second term in the expression (4), is only approximately 5% of total width. In our measurements, we have assumed that A is negligible (see Konjevic [15]), therefore one obtains the following expression:

$$N_e = \left(\frac{\omega}{2\omega_p}\right) \times 10^{16} \quad (5)$$

where ω_p, (in Å), is the Stark broadening parameter of the line, taken from literature [4]: for this study we have selected lines 3854.1 and 4761.1 Å of Pb III, and ω is the FWHM obtained in this work. The calculated electron number density for a temperature of 21,400 K was found to be $7\times10^{16} cm^{-3}$, this obtained value is sufficient to assume LTE. It is well known, for the plasma to be in LTE, atomic and ionic states should be populated and depopulated predominantly by collisions rather than by radiation. This requires that the electron density has to be high enough to ensure a high collision rate. The corresponding lower limit of electron number density is given by McWhirter`s criterion [27]:

$$N_e\left(cm^{-3}\right) \geq 1.6x10^{12}\sqrt{T}\,(\Delta E)^3 \quad (6)$$

where T (in K) is the temperature, ΔE (in eV) is the energy difference between the upper and lower levels of the transition presented in Table 1 and N_e the lower limit of the electron density necessary to maintain the populations of the energy levels at 10% of the LTE by collision, in competition with the radiative processes. In the present case, using the values for the Pb III lines, Table 1, the variation of energy transition ΔE is 1.367 eV and the value of lower limit of electron density as given by Eq. (6) is $5.978\times10^{14} cm^{-3}$.

Table 1
Spectroscopic parameters of Pb III spectra lines using in the determination of the excitation temperature (at 6 Torr atmosphere of argon, delay time of 400 ns, the Pb target having a purity of 99.99%). A_{ij} is the transition probability and E_i is the excited level energy.

Transition	λ (Å)[a]	E_i(eV)	A_{ij} ($\times10^7$ s^{-1})[b]	Error (%)
7p $^3P_0 \rightarrow$ 7s $^3S_1$	4798.6	2.583	15.7 ± 1.7[b]	10.8
7p $^3P_1 \rightarrow$ 7s $^3S_1$	4761.1	2.603	10.3 ± 1.0[b]	9.7
7p $^3P_2 \rightarrow$ 7s $^3S_1$	3854.1	3.216	20.8 ± 2.1[b]	10.0
8s $^3S_1 \rightarrow$ 7p $^3P_1$	3728.7	3.324	14.3 ± 1.5[b]	10.5
7p $^1P_1 \rightarrow$ 7s $^3S_1$	3689.3	3.360	7.0 ± 0.75[b]	11.0
8s $^1S_0 \rightarrow$ 7p $^3P_1$	3530.2	3.511	11.0 ± 1.2[b]	10.9
5f $^3F_3 \rightarrow$ 6d $^3D_2$	3137.8	3.950	34.2 ± 3.6[b]	10.5

[a] NIST [21].
[b] Alonso-Medina [10].

To determine the change of these parameters in different regions of the plasma, their values were obtained at different points using various lines of Pb III, as already indicated in Section 2, deviations from the average are less than (12–15) % for N_e and (5–7) % for T in a region measuring approximately 2 mm in size corresponding to 95% of the emission of light, similar results have been obtained in other LIP experiments [8–11,23]. In this work, the values given for N_e and T correspond to the centre of the plasma.

Finally, great care was taken to minimize the influence of self-absorption on emission line intensities determinations. The absence of self-absorption has been checked using a method described by Thorne [28]. With the aforementioned values of N_e and T we can calculate the absorption coefficient for the studied lines, using the following equation [28], expressed in m^{-1}:

$$k_\omega = \frac{\pi e^2}{2\varepsilon_0 mc} f_{ik} N_i \left[1 - \frac{N_k g_i}{N_i g_k}\right] g(\omega) \quad (7)$$

where f_{ik} is the oscillator strength (absorption), N_k and N_i, the population densities of the lower-level energy and the upper level energy, respectively, were estimated at approximately equal to the electron density, this being an upper limit, g_i and g_j, are statistical weight of state and $g(\omega)$ is the normalized profile of the line. In the maximum, $\omega = 0$, and for a Lorentz profile, $g(o) = 2/\pi\Gamma$, where Γ is the FWHM of the line. A line may be considered optically thin if k_ω (cm^{-1}) × D (cm) ≤ 1 [29]; in present work, D ≈ 1 mm, the value of the optical depth $k_\omega D$ is not more than 0.1. In all the lines studied in this work self-absorption was negligible.

4.2. Stark width of Pb III spectral lines

In this paper, the spectroscopic analysis of the laser-induced plasma emission has provided experimental Stark widths for 25 spectral lines of Pb III at temperature of 21,400 K, and are displayed in column fifth of Table 2, that shows the results parameters normalized to an electron number of 10^{17} cm^{-3}. This data includes new values for 15 emission lines. The first three columns denote the corresponding transition array, the multiplet and the wavelengths (in Å) for each transition; temperatures are indicated in the fourth column. The corresponding errors include uncertainties in the instrumental profile and statistical errors after an average of several spectra with a total of about 100 laser shot. The possible error due to the experimental uncertainty in the density of electrons in this table is not included. In the sixth column the measured Pb III ω values are compared with recent theoretical data calculated based on the semi-classical approach [5] and also taking into account the core polarization (CP) effects [6], and with existing experimental values [4]. It is significant that there is a good agreement between the values [4] and those obtained in this work. It is well known in the literature [15] the existence of certain discrepancies between the experimental measurements of the Stark broadenings and theoretical approaches. As indicated in Ref. [30] there are two problems that can explain the accuracy of the application of semi-empirical impact approximation suggested for Griem [13] in multiply-ionized atoms. The difficulties can be due to the inaccuracy in the used matrix elements or in the Gaunt factors considered. The lack of matrix elements can be the causes that several authors have obtained theoretical values under-estimated when are compared with the experimental ones. In [5,6] the use of a large set of theoretical matrix elements could be an explanation of agreement with our experimental values, apart from few exceptions.

5. Conclusion

Laser-induced plasma spectra from a lead target, having a purity of 99.99%, in a 6 Torr argon atmosphere are recorded with a delay with respect to laser pulse and for a selected interval of time, of 400 ns.

Table 2
Experimental Stark width FWHM, ω (Å), of emission lines of Pb III at a given electron temperature, T(K), and normalized at $N_e = 1.0\times10^{17}$ cm^{-3} (6 Torr of argon, delay time of 400 ns). Line widths are compared with other theoretical and experimental values.

Line No.	Transition array	Multiplet	λ (Å)[a]	T ($\times10^3$ K)	ω (Å) This work	ω (Å) other works
1	7p–8s	$^3P_0$–$^3S_1$	3706.1	21.4	0.91 ± 0.13	
				25.2		1.05[c]
2	7p–8s	$^3P_1$–$^3S_1$	3728.7	21.4	0.94 ± 0.14	
				25.2		1.34[c]
3	7p–8s	$^3P_2$–$^3S_1$	4571.2	21.4	1.96 ± 0.29	
				25.2		2.20[c]
4	7p–8s	$^1P_1$–$^3S_1$	4826.9	21.4	1.61 ± 0.24	
				25.2		1.88[c]
5	7p–8s	$^3P_1$–$^1S_0$	3530.2	21.4	0.60 ± 0.09	
				25.2		0.68[c]
6	7p–8s	$^1P_1$–$^1S_0$	4499.3	21.4	0.98 ± 0.13	
				25.2		0.78[c]
7	7s–7p	$^3S_1$–$^3P_0$	4798.6	21.4	1.09 ± 0.16	
				25.2		1.0 ± 0.2[b], 0.92[c], 0.77[d]
8	7s–7p	$^3S_1$–$^3P_1$	4761.1	21.4	1.01 ± 0.15	
				25.2		1.0 ± 0.2[b], 1.35[c], 1.18[d]
9	7s–7p	$^1S_0$–$^3P_1$	5779.4	21.4	1.79 ± 0.27	
				25.2		2.9 ± 0.6[b], 1.33[c], 1.21[d]
10	7s–7p	$^3S_1$–$^3P_2$	3854.1	21.4	0.82 ± 0.12	
				25.2		0.75 ± 0.16[b], 1.02[c], 0.56[d]
11	7s–7p	$^3S_1$–$^1P_1$	3689.3	21.4	0.69 ± 0.11	
				25.2		0.51[d]
12	7s–7p	$^1S_0$–$^1P_1$	4272.7	21.4	0.42 ± 0.07	
				25.2		0.39[d]
13	6d–7p	$^1D_2$–$^3P_1$	5207.1	21.4	1.89 ± 0.28	
				25.2		2.2 ± 0.6[b], 1.32[c], 1.15[d]
14	6d–7p	$^1D_2$–$^3P_2$	4141.6	21.4	2.23 ± 0.30	
				25.2		2.7 ± 0.6[b], 0.99[c], 0.88[d]
15	6d–7p	$^3D_1$–$^3P_2$	5380.1	21.4	2.00 ± 0.29	
				25.2		2.7 ± 0.7[b], 1.63[d]
16	6d–7p	$^3D_2$–$^3P_2$	5524.0	21.4	2.12 ± 0.31	
				25.2		2.4 ± 0.6[b], 2.5[c], 2.09[d]
17	6d–7p	$^3D_3$–$^3P_2$	5858.0	21.4	1.28 ± 0.20	
				25.2		1.1 ± 0.3[b], 3.3[c], 2.8[d]
18	6d–7p	$^1D_2$–$^1P_1$	3951.9	21.4	0.57 ± 0.09	
				25.2		0.83[d]
19	6d–5f	$^3D_2$–$^3F_3$	3137.8	21.4	0.94 ± 0.14	
				25.2		0.43[d]
20	6d–5f	$^3D_1$–$^3F_2$	3043.8	21.4	0.66 ± 0.10	
				25.2		0.54[d]
21	6d–5f	$^3D_3$–$^3F_4$	3176.5	21.4	1.36 ± 0.26	
				25.2		1.16[d]
22	$6p^2$–7p	$^1D_2$–$^3P_1$	4855.1	21.4	1.45 ± 0.20	
				25.2		1.4 ± 0.4[b], 1.31[c], 1.13[d]
23	5f–5g	$^3F_3$–$^3G_4$	3589.9	21.4	2.68 ± 0.40	
				25.2		3.40[d]
24	5f–5g	$^3F_2$–$^3G_3$	3655.5	21.4	1.14 ± 0.17	
				25.2		2.71[d]
25	5f–5g	$^1F_3$–$^1G_4$	3736.0	21.4	1.52 ± 0.23	
				25.2		3.22[d]

[a] NIST [21].
[b] Alonso-Medina and Colón [4].
[c] Alonso-Medina et al. [5].
[d] Zanón et al. [6].

Spectroscopic analysis of the plasma light emission has provided the experimental Stark widths for 25 emission lines of Pb III. For 15 of these emission lines, no experimental values of Stark widths have been reported by other authors. No self-absorption effects have been detected.

The temperature of the plasma (21,400 K) has been determined from the Boltzmann plot method using the relative emission line intensities of Pb III and from Saha's equation, where the electron number density (7×10^{16}cm^{-3}) was estimated from the Stark broadening.

Acknowledgements

This work was supported by the project “MAT2008-02704/MAT” funded by the Spanish Ministry of Science and Technology.

References

[1] D.S. Leckrone, C.R. Proffitt, G.M. Wahlgren, S.G. Johansson, T. Brage, Very high resolution UV spectroscopy of a chemically peculiar: results of the χ Lupi pathfinder project, ApJ. 117 (1999) 1454–1470.
[2] G. Wahlgren, J. Zverko, W.W. Weiss, J. Ziznosky, S.J. Adelman, Observations of nonmagnetic CP stars: Crossing boundaries, eds, Proc. IAU Symp. 224, The A-Star Puzzle, Kluwer, Dordrecht, 2004.
[3] P. Chayer, M. Fontaine, G. Fontaine, F. Wesemael, F. Dupuis, *Fuse* observations of germanium, zirconium and lead in sdB stars, Baltic Astronomy 15 (2006) 131–138.
[4] A. Alonso-Medina, C. Colón, Stark widths of several Pb III spectral lines in a laser-induced lead plasma, Astron. Astrophys. 466 (2007) 399–403.
[5] A. Alonso-Medina, C. Colón, A. Zanón, Theoretical study of the Stark width and shift parameters of Pb III lines: predictions and regularities, Mon. Not. R. Astron. Soc. 385 (2008) 261–268.
[6] A. Zanón, A. Alonso-Medina, C. Colón, Core-polarization effects for the Stark Broadening of Pb III spectral lines: predictions and regularities, Int. Rev. At. Mol. Phys. 1 (2010) 1–11.
[7] H.R. Griem, Principles of Plasma Spectroscopy, Cambridge University Press, 1997.
[8] A. Alonso-Medina, Experimental determination of the Stark widths of Pb I spectral lines in a laser induced plasma, Spectrochim. Acta Part B 63 (2008) 598–602.
[9] A. Alonso-Medina, A spectroscopic study of laser-induced tin-lead plasma: transition probabilities for spectral lines of Sn I, Spectrochim. Acta Part B 65 (2010) 158–166.
[10] A. Alonso-Medina, Experimental transition probabilities for several spectral lines arising from $5d^{10}$ 6s{8s, 7p, 5f, 5g} electronic configurations of Pb III, J. Quant. Spectrosc. Radiat. Transfer 111 (2010) 2043–2051.
[11] A. Alonso-Medina, Probabilidades de transición en átomos pesados: aplicación al talio y al plomo. Razones de ramificación y momentos electrónicos de transición en la molécula de plata. Ph.D. Thesis (1995). Eindhove University Complutense of Madrid, Spain (2001): oai: www.ucm.es:1927. ISBN:84-669-0380-1.
[12] W. Lochte-Hotgreven, Plasma diagnostics. North-Holland; WLochte-Holtgreven, Amsterdam, 1968.
[13] H.R. Griem, Plasma Spectroscopy, McGraw Hill, New York, 1964.
[14] H.R. Griem, Spectral Line Broadening by Plasma, Academic Press, New York, 1974.
[15] N. Konjevic´, Plasma broadening and shifting of non-hydrogenic spectral lines: present status and applications, Phys. Rep. 316 (1999) 339–401.
[16] A.W. Ali, H.R. Griem, Theory of resonance broadening of spectral lines by atom-atom impacts, Phys. Rev. 140 (1965) A1044–A1048.
[17] S. Djurović, N. Konjević, On the use of non-hydrogenic spectral lines for low electron density and high pressure plasma diagnostics, Plasma Sources Sci. Technol. 18 (2009) 035011 (8pp).
[18] M. Baranger, Atomic and Molecular Processes, Academic, New York, 1962.
[19] G. Befeki, Principles of Laser Plasmas, Wiley Interscience, New York, 1976.
[20] G. Cristoforetti, A. De Giacomo, M. Dell'Aglio, S. Legnaioli, E. Tognoni, V. Palleschi, N. Omenetto, Local thermodynamic equilibrium in laser-induced plasma breakdown spectroscopy: beyond the McWhirter criterion, Spectrochim. Acta Part B 65 (2010) 86–95.
[21] http://physics.nist.gov/PhysRefData/Handbook/index.html.
[22] C.E. Moore, Atomic Energy Levels NBS 467 vol III, U.S.GPO, Washington D.C, 1958, p. 208.
[23] A. Alonso-Medina, Transition probabilities of 30 Pb II lines of the spectrum obtained by emission of a laser-produced plasma, Phys. Scr. 55 (1997) 49–53.
[24] A. Alonso-Medina, Transition probabilities for several UV lines of Pb II, J. Quant. Spectrosc. Radiat. Transfer 55 (1996) 151–154.
[25] V. Milosavljevic, G. Poparic, Atomic spectral line free parameter deconvolution procedure, Phys. Rev. 63 (2001) 036404–036407.
[26] P.J. Wolf, The plasma properties of laser-ablated SiO_2, J. Appl. Phys. 72 (1992) 1280–1289.
[27] R.W.P. McWhirter, in: R.H. Huddlestone, S.L. Leonard (Eds.), Plasma Diagnostic Technics, Academic, New York, 1963.
[28] A.P. Thorne, Spectrophysics, 2nd edition Chapman and Hall, London, 1988.
[29] A. Corney, Atomic and Laser Spectroscopy, Oxford University Press, 1977.
[30] M.S. Dimitrijecic, N. Konjevic´, Stark broadening of doubly and triply ionized atoms, J. Quant. Spectrosc. Radiat. Transfer 24 (1980) 451–459.